

A local non-iterative method for the implementation of Procrustean entanglement distillation.

D. R. M. Arvidsson-Shukur, E. T. Owen, and C. H. W. Barnes

Cavendish Laboratory, Department of Physics, University of Cambridge, Cambridge CB3 0HE, United Kingdom

(Dated: March 8, 2016)

We present a local non-iterative method for the implementation of Procrustean entanglement distillation on a pair of entangled qubits using a positive-operator-valued measure (POVM). We show that this POVM can be applied equally to massless and massive qubits in hybrid quantum systems. For massless particles we consider single photons, for which the POVM can be implemented using standard linear optics components. For massive particles, we consider spin- $\frac{1}{2}$ qubits. Numerical solutions to the time-dependent Schrödinger equation allow us to tailor a Hamiltonian for gaussian wavepackets to implement the POVM on these qubits. Our non-iterative method can be applied, not only to pure ensembles with particle pairs of known identical entanglement, but also to ensembles of particle pairs with a distribution of different entanglement entropies. The outlined protocol eases the requirement for the creation of m -particle cluster states for measurement based quantum computing, such that the resource states can have entropies of entanglement approaching zero as $\mathcal{O}(1/\text{poly}(m))$.

PACS numbers: 03.65.Ud, 03.67.Ac, 03.67.Dd, 05.60.Gg, 42.50.Ex, 41.85.Ct

The number of potential disruptive technologies that require quantum entanglement has gradually risen over the last three decades [1–7]. Two main themes run through these technologies: large scale quantum computing, which, at present, exists purely on a theoretical level [1, 5, 8–12]; and quantum cryptography, which is now on the verge of widespread commercial application [2, 13–16]. However, the issue of quantum decoherence naturally raises the question of what the limit on practical applications with controlled entanglement in future technologies will be [17]. The crucial question is whether quantum error correction [18–22], entanglement purification [23–25], and entanglement distillation [26, 27], which respectively—as their names suggest—correct, purify and distill entanglement, can be applied on a large scale and in a practical manner to all parts of a quantum system in order to make protocols robust against noisy environments or non-ideal quantum hardware.

Non-locality—inherent to entangled states—is used in quantum cryptography schemes with massless particles, to gain significant benefits over schemes without entanglement [28–31]. For example, Ekert’s protocol, which utilises entangled pairs of photons, allows a key to remain undefined until the communicating parties carry out their measurements [2, 32]. The requirement on the initial particle pairs to be Bell states can be removed by using local entanglement distillation in conjunction with this protocol.

Furthermore, entanglement is a crucial resource for large-scale fault-tolerant quantum computing [33] with massive particles. For example, measurement-based quantum computing (MBQC) [34, 35] could potentially be realised with clusters of trapped atoms.[36] As we will show, requirements on the initial entanglement of the spins can again be relaxed through the application of local entanglement distillation.

One of the most significant breakthroughs in en-

tanglement distillation has been Bennett’s Procrustean method, where a subset of qubit pairs in pure states is discarded, whilst harnessing their entanglement, making the remaining ensemble of pairs more entangled [26]. Significantly, Bennett’s method can be *local* in that, it allows entanglement distillation to occur through single qubit operations on only one of the particles in a two-particle pair. Experimental difficulties in applying a great number of operations are reduced by the *non-iterative* nature of this scheme. The unitary quantum evolution operations can theoretically be carried out in a straightforward manner using a positive-operator-valued measure (POVM).

In terms of quantum hardware, this POVM will need to be tailored to the specific qubit being manipulated: the spatial quantum evolution of massless particles is essentially non-dispersive, but interactions between particles are weak; whilst spatial evolution of massive particles is dispersive, but interactions can be strong. This presents a challenge because most future quantum technologies will be hybrid quantum systems, utilising different physical qubits to carry out specific tasks in an integrated system [37–40]. For example, entanglement can be created between trapped ions, distributed with photons and stored using electron spins. Considering an Ekert-type cryptography protocol [2], in which Alice only possesses weakly entangled photon pairs: If the qubit storage capacity of Bob is low, it is beneficial to carry out entanglement distillation on the photonic states prior to the entanglement transfer to the massive storage qubits. However, if Bob’s storage capacity is good, it is beneficial to leave the entanglement distillation to be carried out on Bob’s massive storage qubits until just before the key is to be read out, as it would—in the case of a burglar attack [28]—increase the efforts required by an untrusted party to gain information. We therefore outline our method for local entanglement distillation, which has applications for precisely these problems, addressing both massless and

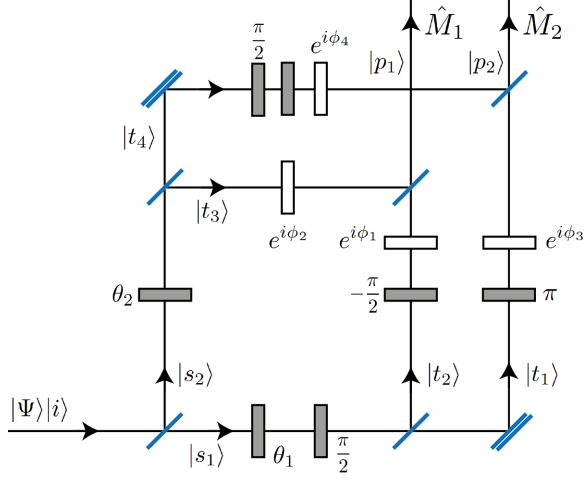


FIG. 1. AP POVM from reference [41]. Qubit rotations of the POVM are denoted by shaded rectangles, the phase shifts by open rectangles and the spatial degrees of freedom by the states $|i\rangle$, $|s_{1,2}\rangle$, $|t_{1,2,3,4}\rangle$ or $|p_{1,2}\rangle$. Single and double diagonal lines indicate polarizing beam-splitters and reflecting mirrors respectively.

massive particles.

In this letter, we present a new practical method to implement Procrustean entanglement distillation using a local POVM. Our method can be applied equally to quantum degrees of freedom of massless and massive particles in pure states. The method relies on a knowledge of the initial state, but we show that it can also be applied to ensembles of pure particle pairs with a distribution of entropies of entanglement. We show how the protocol can be used to enable the creation of clusters for MBQC as well as for realising quantum cryptography, using vanishingly weak entanglement resources, thus substantially reducing the requirements on the resource states in such operations.

In order to achieve compatibility with hybrid quantum systems, we implement our local POVM using the Anherst and Payne (AP) double interferometer device from reference [41] shown in FIG. 1. This device requires a bipartite input form consisting of a qubit state $|\Psi\rangle = \alpha|0\rangle + \beta|1\rangle$ and a spatial degree of freedom. The action of the AP POVM on the input state $|\Psi\rangle|i\rangle$ is to create two spatially decoupled output states $|\Psi_i\rangle|p_i\rangle = \hat{M}_i|\Psi\rangle|p_i\rangle / \sqrt{\langle\Psi|\hat{M}_i^\dagger\hat{M}_i|\Psi\rangle}$, where:

$$\hat{M}_1 = \cos(\theta_1)e^{i\phi_1}|0\rangle\langle 0| + \cos(\theta_2)e^{i\phi_2}|1\rangle\langle 1|, \quad (1)$$

$$\hat{M}_2 = \sin(\theta_1)e^{i\phi_3}|0\rangle\langle 0| + \sin(\theta_2)e^{i\phi_4}|1\rangle\langle 1|. \quad (2)$$

In FIG. 1 the qubit rotations of the AP POVM are denoted by shaded rectangles, the phase shifts by open rectangles and the spatial degrees of freedom by the states $|i\rangle$, $|s_{1,2}\rangle$, $|t_{1,2,3,4}\rangle$ or $|p_{1,2}\rangle$.

For the weakly entangled state,

$$|\Psi_{A,B}\rangle = \alpha|0_A\rangle|0_B\rangle + \beta|1_A\rangle|1_B\rangle, \quad (3)$$

shared between say Alice and Bob, Procrustean entanglement distillation can be achieved by applying the AP POVM to just Alice's particle, A . The parameters for the POVM can be defined in terms of an angle, φ , and a phase, γ . For a known initial state of the form of Eq. 3 we can set these parameters such that $\alpha = \cos(\varphi)$ and $\beta = \exp(i\gamma)\sin(\varphi)$. We then set $\phi_{2,3} = -\gamma$, $\phi_{1,2} = 0$, $\theta_1 = \Re[\arccos(\tan(\varphi))]$ and $\theta_2 = \Re[\arccos(\cot(\varphi))]$. We see that Alice's output in $|p_1\rangle$ is acted upon by $\hat{M}_1^A = \tan(\varphi)|0\rangle\langle 0| + |1\rangle\langle 1|$ if $l\pi - \pi/4 \leq \varphi \leq l\pi + \pi/4$ (for some integer l) and $\hat{M}_1^A = |0\rangle\langle 0| + \cot(\varphi)|1\rangle\langle 1|$ otherwise. If we pass Alice's initial state, $|\Psi_A\rangle$, through such a POVM, the two-particle state will, with probability $P_1 = 1 - |\cos(2\varphi)|$, be output as $|\Psi_1\rangle = \frac{1}{\sqrt{2}}(|1_A\rangle|1_B\rangle + |0_A\rangle|0_B\rangle)$, which is a maximally entangled state.

We have effectively established a way for Alice and Bob to *locally* distill their entanglement by letting one of them pass her/his ensemble of particles through the device in FIG. 1 and then classically communicate to their partner which particles to discard.[26] The successful creation of a Bell state at the p_1 -output is heralded by the lack of detection of a particle at the p_2 -output.

We also note that, after a successful distillation, the weakly entangled n -particle state

$$|\Phi\rangle = \alpha|0\rangle^{\otimes n} + \beta|1\rangle^{\otimes n}, \quad (4)$$

will be output as a GHZ state if any one of the particles is sent through the POVM device, irrespective of the value of n .

If we consider the photonic case, $|\Psi_{A,B}\rangle = \alpha|H_A\rangle|H_B\rangle + \beta|V_A\rangle|V_B\rangle$, the unitary transformations of the POVM can be implemented in a straightforward manner. The polarization rotations can be applied by wave plates and the phase-shifts can be induced by electro-optical phase modulators. The spatial evolution can be controlled by the use of mirrors and polarizing beam-splitters.

We will now adapt our method to enable distillation of massive spin- $\frac{1}{2}$ states so that it can be used in hybrid quantum systems. The application of the optical unitary transformations to pure massive particle joint states is not straightforward. Whilst a photon can pass through free space without dispersing significantly, the wavefunction of a massive particle—such as an ion or an electron—will disperse in a much more uncontrolled manner. Hence, even a simple structure such as a Mach-Zehnder Interferometer (MZI), becomes non-trivial to execute. FIG. 2 shows a massive wavepacket, passing through a MZI. (For numerical methods see Supplementary Materials). Spin-dependent beam-splitters are inserted at the junctions. Even if the device curvature, wavepacket shape and momentum distribution are chosen optimally, the probability density disperses to unwanted locations of the MZI. This dramatically reduces the fidelity of the qubit operation.

The dispersion of the states can be eliminated through the use of Gaussian wavepackets in harmonic confining

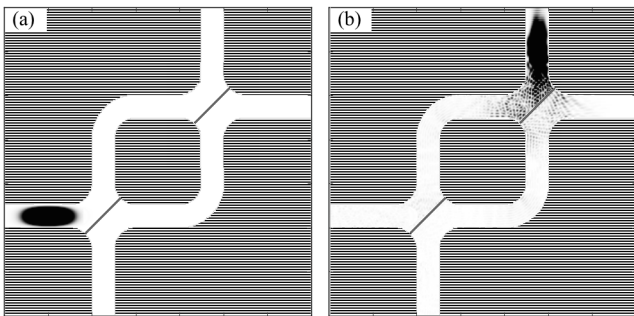


FIG. 2. Mach-Zehnder Interferometer for massive particles at two different time steps. The potential is infinite in the striped area and zero elsewhere. The beam-splitters of the MZI are indicated with grey diagonal lines.

potentials [42, 43]. Such potentials have been implemented successfully in ion traps [44–46] and equivalent potentials can be achieved for electrons in semiconductor quantum devices using Schottky surface gates.[47–50] The polarization rotations and phase shifts (indicated in FIG. 1) for spin- $\frac{1}{2}$ particles are described by unitary operators of the form:

$$\hat{R}_k = \mathcal{T} \exp [i\lambda(t)\sigma_k t], \quad (5)$$

where $\lambda(t)$ is some time-dependent strength parameter and σ_k is a Pauli matrix with $k = x, y, z$. Such unitary evolution can be realised through the Zeeman effect $\hat{H}_{rot} = -\boldsymbol{\mu} \cdot \mathbf{B}(t)$, where $\boldsymbol{\mu}$ is the magnetic dipole moment of the particle and $\mathbf{B}(t)$ is the magnetic field, which we take to be uniform in each spatial dimension over the particle wavepacket. Spin-selective beam-splitters can be produced by including a spin-dependent shift to the minimum of the harmonic confining potential. The initial harmonic potential (in 2D) would be given by $V(y, z) = \frac{1}{2}m\omega^2(y^2 + z^2)$. The shift required for the spin-dependent transport can then be imposed by diabatically or adiabatically applying a field coupled to the spin degree of freedom (e.g. a magnetic field $B_z = B_0 z$ for some constant B_0) together with a uniform electric field, E_0 , such that:

$$V(y, z) = \frac{1}{2}m\omega^2 \left(y^2 + z^2 \pm \frac{2\mu}{\omega^2 m} B_0 z + \frac{2E_0 q}{m\omega^2} \right) \quad (6)$$

$$= \frac{1}{2}m\omega^2 (y^2 + (z \pm z_1)^2), \quad (7)$$

where $z_1 \equiv \mu B_0 / (\omega^2 m)$, $E_0 \equiv (z_1 \omega)^2 m / (2q)$, μ is the strength of the magnetic moment and q is the charge on the particle. The direction of the transport will thus be determined by the spin of the particle, hence a spin-selecting beam-splitter. For electrons, spin-selective beam-splitters can alternatively be created by allowing the wavepacket to fall into a potential with its minimum situated at the mid-point of a narrow magnetic semiconductor barrier (working as a spin-filter) [51], avoiding the careful manipulation of magnetic fields.

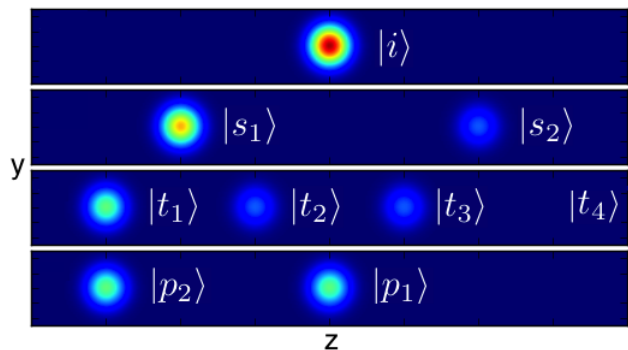


FIG. 3. Probability distribution of a spin- $\frac{1}{2}$ particle going through the four stages of FIG. 1.

Our simulations confirm that the required spatial translations can be obtained by imposing either diabatic or adiabatic (as in [8]) potential fields. However, minor disturbances to the translations are introduced if adiabatic potentials with reasonable experimental time-scales are used. Hence, diabatic changes, if attainable, are preferred in order to increase the fidelity of the unitary transformations in the POVM.

Using these single-qubit operations, the implementation of our POVM for spin- $\frac{1}{2}$ particles can now be simulated using the *same* parameters as we have used for the optical case. The evolution of the wavefunction probability distribution in the POVM is shown in FIG. 3: one particle from a joint initial spin-state, $|\Psi_{A,B}\rangle = \cos(30^\circ)|\downarrow_A\rangle|\downarrow_B\rangle + i\sin(30^\circ)|\uparrow_A\rangle|\uparrow_B\rangle$, is sent through the POVM to create a Bell state. The spatial degree of freedom is labelled as in Fig 1. Significantly, by using gaussian wavepackets, the POVM can be implemented with a fidelity of better than 99.5%. For more detailed descriptions of the time evolution, see Supplementary Materials.

We have now shown how our POVM can be implemented using both photonic and spin- $\frac{1}{2}$ qubits. The crucial assumption of the Procrustean distillation protocol though, is that the initial pure state is exactly known. However, experimentally, the process producing the weakly entangled states is more likely to produce an ensemble of particle pairs with a distribution of entanglement strengths, based on the entropy of entanglement. Our simulations show that our POVM can also be applied to such ensembles. We consider it sufficient for the final ensemble to have a higher mean entropy of entanglement than the initial one. By selecting a subset of the particles from the ensemble, one can optimise the POVM configuration, consuming these particles. Then the remaining ensemble can pass through the optimised POVM.

In FIG. 4 we show the entropy of entanglement of particles in the initial and the final ensembles. FIG. 4(a) shows the change in mean entropy of entanglement, $\Delta\bar{S}$, as a function of initial mean entropy, \bar{S}_{in} , and POVM angle, φ , as previously related to θ_1 and θ_2 . Further-

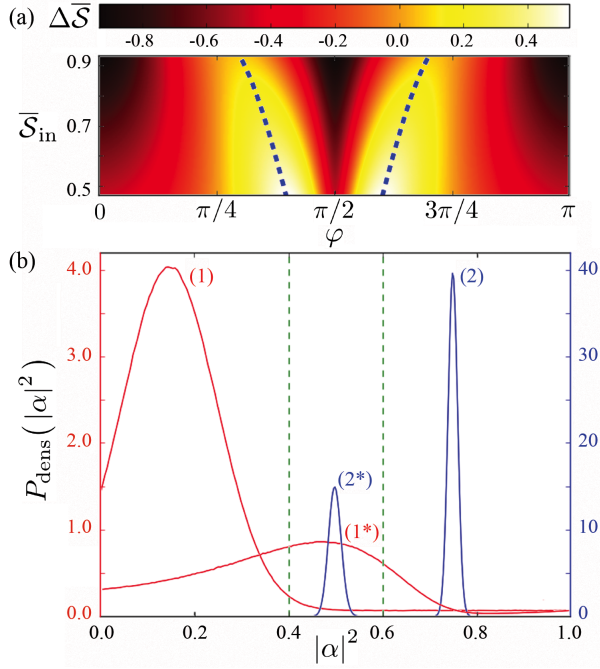


FIG. 4. (color online) (a) Difference between the initial and the final ensemble mean entropy of entanglement (contour from color-bar). The horizontal axis shows the POVM parameter, φ , and the vertical axis shows the initial mean value of the entropy of entanglement. (b) Probability density as a function of $|\alpha|^2$, of two example input distributions, (1) and (2), and their corresponding non-normalized $|p_1\rangle$ output distributions, (1*) and (2*).

more, the value of $|\alpha|^2$ (the probability of state $|0\rangle$) of the initial ensemble was assumed to have a Gaussian profile with a narrow width of $\sigma = 0.01$. The dotted line shows the locus of the optimal POVM angle for ensembles of identical pairs. We found that the lower the initial mean entanglement is, the higher the possible increase of mean entanglement can be. The simulations were carried out using Monte Carlo theory with an ensemble size of 10^5 particles in each distribution. Simulations show that for many well-behaved distributions our setup could efficiently produce a final ensemble of increased average entanglement.

As stated, many of the promising quantum technologies, such as quantum cryptography or MBQC, depend on the possession of pure maximally entangled states [2, 52, 53]. One could thus be inclined to consider maximally entangled states as a crucial resource for many quantum processes of interest. We show how our protocol can be used to ease the requirements on the resource states of, for example, MBQC.

It has been shown [52] that cluster states for universal MBQC can be created using only Bell states for boosted Type II fusion gates [53, 54] and 3-qubit GHZ states. For a computational depth (related to the number of qubits on a single line of MBQC code), k , linear lattice dimension, L , and number of logical qubits, n , the number of 3-

particle GHZ states needed to create the cluster state for the computation is of the order $\mathcal{O}(n \cdot k \cdot L^3)$. [52] The number of Bell states needed scales linearly with the number of GHZ states used.

Say that we only have access to states of the form $|\psi\rangle_3 = \alpha|000\rangle + \sqrt{1-\alpha^2}|111\rangle$ and $|\psi\rangle_2 = \alpha|00\rangle + \sqrt{1-\alpha^2}|11\rangle$. If α approaches zero as $\mathcal{O}(1/\text{poly}(n \cdot k \cdot L^3))$ then so does the entropy of entanglement. The probability of distilling these states scales quadratically with α . Hence, the number of particles needed to ensure a successful distillation process would scale by the order of $\mathcal{O}(1/\alpha^2)$, i.e. polynomially. Each distillation process itself requires a constant number of unitary 1-qubit operations. Hence, in order to produce the cluster state from ensembles of two and three particle states of entanglement approaching zero polynomially, one would have to have an ensemble size of the polynomial order $\mathcal{O}(n \cdot k \cdot L^3/\alpha^2)$ and an addition of a polynomial number of unitary single qubit operations as compared to the method described in [53], keeping the possibility to solve **BQP** problems in polynomial time. We thus see that, with a polynomial increase in initial resources, cluster states for MBQC can be formed with ensembles of polynomially vanishing entropy of entanglement, without introducing additional multi-qubit operations.

With the result above, it also becomes obvious that quantum cryptography based on entanglement can be carried out even if the particle pairs have polynomially vanishing entanglement. The only requirement being that the number of particles used in the protocol increases polynomially.

In conclusion, we have described a local non-iterative implementation of Procrustean entanglement distillation on a pair of entangled qubits using a POVM. For massless particles the protocol is implemented by realising the AP double interferometer POVM [41] with standard optical components. For massive spin- $\frac{1}{2}$ particles, the POVM is realised by the spatial and spin-dependent quantum evolution induced by adiabatic or diabatic changes to magnetic fields and electric harmonic potentials. By virtually eliminating the dispersion of the massive wavepackets, this interestingly allows the simplicity of the double interferometer to be transferred to the massive case. Owing to the difficulty of controlling photon-photon interactions, linear-optics-like processing of massive (more easily interacting) particles should be valuable for quantum computational aspirations or quantum cryptography with hybrid systems. Our Monte-Carlo based numerical investigation shows how the protocol can increase the average entropy of entanglement of particle pair ensembles with distributions of entanglement entropies. This should be beneficial for quantum error correction schemes, which only require that the average level of qubit errors in the ensemble is below some limiting value.[18] Finally, by comparison with works on the creation of cluster states for MBQC,[52–54] we show that the efficiency of the distillation protocol is sufficient to allow the entanglement of the MBQC resource states to decrease polynomially to

zero.

The authors would like to express their gratitude towards Charles Bennett and Richard Jozsa for helpful discussions. This work was supported by the EPSRC, Cambridge Laboratory of Hitachi Limited via Project for Developing Innovation Systems of the MEXT in Japan, Tornspiran's Trust Fund, Lars Hierta's Memorial Foundation, Långmanska kulturfonden's Trust Fund, Sixten Gemzeus' Fund and Anna Whitlock's Fund.

I. SUPPLEMENTARY MATERIAL

A. Numerical Methods

In order to obtain the results of this letter, the time-dependent Schrödinger equation (TDSE) was solved:

$$\hat{H}\Psi(\bar{r}, t) = i\hbar\partial_t\Psi(\bar{r}, t), \quad (8)$$

where $\hat{H} = -\frac{\hbar^2}{2m}\nabla^2 + \hat{V}(\bar{r}, t)$ is the space and time dependent Hamiltonian of the system and $\Psi(\bar{r}, t)$ is the wavefunction.

The spatial domain of the wavefunction is discretised using a finite difference method (as in [55]) and the temporal domain is discretised into equally spaced points.

The second order derivative of the kinetic term can be expanded as:

$$\nabla^2\Psi(x, y, z) = \quad (9)$$

$$\frac{\Psi(x + \Delta x) - 2\Psi(x) + \Psi(x - \Delta x)}{\Delta x^2} \quad (10)$$

$$+ \frac{\Psi(y + \Delta y) - 2\Psi(y) + \Psi(y - \Delta y)}{\Delta y^2} \quad (11)$$

$$+ \frac{\Psi(z + \Delta z) - 2\Psi(z) + \Psi(z - \Delta z)}{\Delta z^2}. \quad (12)$$

We follow ref. [55, 56] and rewrite our wavefunction with a discretised notation:

$$\Psi(x = k\Delta x, y = l\Delta y, z = m\Delta z, t = n\Delta t) \equiv \psi_{k,l,m}^n.$$

The 3D time-dependent potential can also be discretised on these points: $V(k\Delta x, l\Delta y, m\Delta z, n\Delta t) \equiv V_{k,l,m}^n$. By generalising the methods from ref. [56] to 3D we can then write our Hamiltonian as:

$$H\psi_{k,l,m}^n = \quad (13)$$

$$\frac{\hbar^2}{2m} \left(\frac{2\psi_{k,l,m}^n - \psi_{k+1,l,m}^n - \psi_{k-1,l,m}^n}{\Delta x^2} \right) \quad (14)$$

$$+ \frac{2\psi_{k,l,m}^n - \psi_{k,l+1,m}^n - \psi_{k,l-1,m}^n}{\Delta y^2} \quad (15)$$

$$+ \frac{2\psi_{k,l,m}^n - \psi_{k,l,m+1}^n - \psi_{k,l,m-1}^n}{\Delta z^2} \Big) + V_{k,l,m}^n \psi_{k,l,m}^n \quad (16)$$

The time evolution of the wavefunction can be approximated by solving the discretised Schrödinger equation [56]:

$$\psi_{k,l,m}^{n+1} = \exp(-i\Delta t H/\hbar) \psi_{k,l,m}^n \quad (17)$$

$$\approx (1 - i\Delta t H/\hbar) \psi_{k,l,m}^n. \quad (18)$$

This method is, however, not be stable [57], and we proceed by the following step:

$$\psi_{k,l,m}^{n+1} - \psi_{k,l,m}^{n-1} \approx -(2i\Delta t H/\hbar) \psi_{k,l,m}^n. \quad (19)$$

Substituting the Hamiltonian from above and rearranging we find that:

$$\psi_{k,l,m}^{n+1} \approx \psi_{k,l,m}^{n-1} + \left(\frac{-2i\Delta t}{\hbar} \right) V_{k,l,m}^n \psi_{k,l,m}^n \quad (20)$$

$$+ \frac{i\hbar\Delta t}{m} \left[\frac{2\psi_{k,l,m}^n - \psi_{k+1,l,m}^n - \psi_{k-1,l,m}^n}{\Delta x^2} \right] \quad (21)$$

$$+ \frac{2\psi_{k,l,m}^n - \psi_{k,l+1,m}^n - \psi_{k,l-1,m}^n}{\Delta y^2} \quad (22)$$

$$+ \frac{2\psi_{k,l,m}^n - \psi_{k,l,m+1}^n - \psi_{k,l,m-1}^n}{\Delta z^2} \Big]. \quad (23)$$

This method is sufficient to solve the TDSE.[58] However, a more accurate solution can be obtained by separating the wavefunction into its real and imaginary component, $\psi_{k,l,m}^n = u_{k,l,m}^n + i v_{k,l,m}^n$, where we evaluate the imaginary component at a staggered time as compared to the real component: $n' = n + 1/2$. [58]

Finally, we extend the methods of refs. [56, 58] further by including a spin-dependent component such that the potential takes the form of:

$$V_{k,l,m}^n \rightarrow V_{k,l,m}^n + \sum_{i,j=\uparrow,\downarrow} V_{k,l,m,(i,j)}^n, \quad (24)$$

where $V_{k,l,m,(i,j)}^n$ is the coefficients of the spin-dependent part of the potential that acts on the wavefunction of spin j rotating it to spin i . It should be noted that the Lorentz term is negligible for scenarios considered in this letter, such that the spin-component could be introduced as an additional term in the potential.

The algorithm then performs the following iteration:

$$\begin{aligned} u_{k,l,m,i=\uparrow,\downarrow}^{n+1} &\approx u_{k,l,m,i}^{n-1} + \left(\frac{2\Delta t}{\hbar} \right) V_{k,l,m,i}^n v_{k,l,m,i}^n \\ &+ \frac{\hbar\Delta t}{m} \left[\frac{2v_{k,l,m,i}^n - v_{k+1,l,m,i}^n - v_{k-1,l,m,i}^n}{\Delta x^2} \right. \\ &+ \frac{2v_{k,l,m,i}^n - v_{k,l+1,m,i}^n - v_{k,l-1,m,i}^n}{\Delta y^2} \\ &+ \left. \frac{2v_{k,l,m,i}^n - v_{k,l,m+1,i}^n - v_{k,l,m-1,i}^n}{\Delta z^2} \right] \\ &+ \left(\frac{2\Delta t}{\hbar} \right) \sum_{j=\uparrow,\downarrow} \Im(V_{k,l,m,(i,j)}^n) u_{k,l,m,j}^n \\ &+ \left(\frac{2\Delta t}{\hbar} \right) \sum_{j=\uparrow,\downarrow} \Re(V_{k,l,m,(i,j)}^n) v_{k,l,m,j}^n, \end{aligned}$$

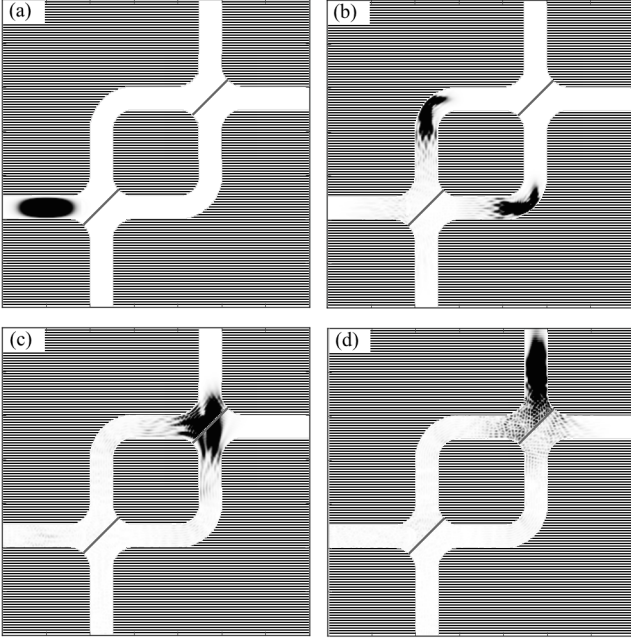


FIG. 5. 2D simulation of Mach-Zehnder Interferometer for massive particles at four different time steps. The potential is infinite in the striped area and zero elsewhere. The beam-splitters of the MZI are indicated with grey diagonal lines.

for the real part and

$$\begin{aligned}
 v_{k,l,m,i=\uparrow,\downarrow}^{n'+1} &\approx v_{k,l,m,i}^{n'-1} - \left(\frac{2\Delta t}{\hbar}\right) V_{k,l,m,i}^n u_{k,l,m,i}^n \\
 &- \frac{\hbar\Delta t}{m} \left[\frac{2u_{k,l,m,i}^n - u_{k+1,l,m,i}^n - u_{k-1,l,m,i}^n}{\Delta x^2} \right. \\
 &\quad + \frac{2u_{k,l,m,i}^n - u_{k,l+1,m,i}^n - u_{k,l-1,m,i}^n}{\Delta y^2} \\
 &\quad \left. + \frac{2u_{k,l,m,i}^n - u_{k,l,m+1,i}^n - u_{k,l,m-1,i}^n}{\Delta z^2} \right] \\
 &+ \left(\frac{2\Delta t}{\hbar}\right) \sum_{j=\uparrow,\downarrow} \Im(V_{k,l,m,(i,j)}^n) v_{k,l,m,j}^n \\
 &- \left(\frac{2\Delta t}{\hbar}\right) \sum_{j=\uparrow,\downarrow} \Re(V_{k,l,m,(i,j)}^n) u_{k,l,m,j}^n
 \end{aligned}$$

for the imaginary part. If the greatest eigenvalue of the Hamiltonian is E_{max} , then the time-step has to satisfy $\Delta t < E_{max}/\hbar$ for the solution to be stable.[56] This algorithm provides an excellent way of obtaining stable solutions to the TDSE using GPU boosted code.

B. Quantum Evolution of Massive Particle POVM

In the following section we describe the quantum evolution of Alice's particle from the initial spin-state, $|\Psi_{A,B}\rangle = \cos(30^\circ)|\downarrow_A\rangle|\downarrow_B\rangle + i\sin(30^\circ)|\uparrow_A\rangle|\uparrow_B\rangle$, when it is sent through our protocol. As can be seen in Fig. 5, a non-dispersive unitary evolution of high fidelity is

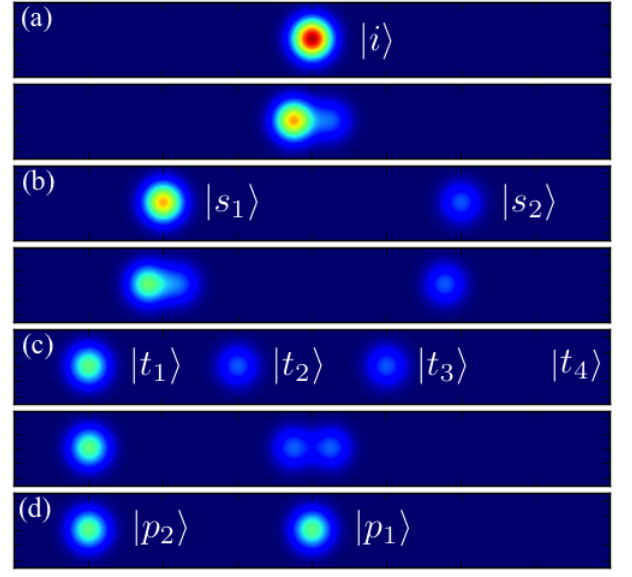


FIG. 6. (color online) Probability distribution of a spin- $\frac{1}{2}$ particle going through the stages of the setup of FIG. 1. The initial $|i\rangle|\Psi\rangle$ state is evolved to $|p_1\rangle\hat{M}_1|\Psi\rangle + |p_2\rangle\hat{M}_2|\Psi\rangle$.

not possible with an optics-like MZI device. Hence, a time-dependent Hamiltonian has to be tailored from the methods described in the letter. The spatial degree of freedom is, as in ref. [41], labelled by $|i\rangle$, $|s_{1,2}\rangle$, $|t_{1,2,3,4}\rangle$ and $|p_{1,2}\rangle$. The labels are used as subscripts for the spin wavefunction indicating the respective evolutions of FIG. 1.

At FIG. 6(a) Alice's particle enters the POVM as $|\Psi\rangle|i\rangle$ in FIG. 1. It is held at the bottom of a harmonic potential created by an electric field. A spin-dependent shift to the minimum of the potential well is imposed as by Eq. 6. This causes the wavefunction to split into its spin components, $|\Psi_{s_1}\rangle|s_1\rangle$ and $|\Psi_{s_2}\rangle|s_2\rangle$, and evolve to FIG. 6(b).

In FIG. 6(b) $|\Psi_{s_1}\rangle|s_1\rangle$ and $|\Psi_{s_2}\rangle|s_2\rangle$ are trapped by separate harmonic potentials created by electric fields. The different unitary rotations of FIG. 1 can then be applied to the respective parts of the wavefunction as by Eq. 5. After that, a spin-dependent shift of the potential wells at $|s_1\rangle$ and $|s_2\rangle$ is applied using the method of Eq. 6 at both locations. This causes the wavefunction to evolve into the configuration at FIG. 6(c) with $|\Psi_{t_1}\rangle|t_1\rangle$, $|\Psi_{t_2}\rangle|t_2\rangle$ and $|\Psi_{t_3}\rangle|t_3\rangle$ ($|\Psi_{t_4}\rangle|t_4\rangle$ having zero probability of occupation).

In FIG. 6(c) the three parts of the wavefunction are trapped in three electric field harmonic potential wells. Again, the respective spin rotations and phase shifts are applied. Then the potentials of the two parts in the middle ($|t_2\rangle$ and $|t_3\rangle$) are shifted as by Eq. 6. This causes $|\Psi_{t_2}\rangle|t_2\rangle$ and $|\Psi_{t_3}\rangle|t_3\rangle$ to interfere constructively in FIG. 6(d) and form $|\Psi_{p_1}\rangle|p_1\rangle$ whilst $|t_1\rangle$ is re-labelled as $|p_2\rangle$. $|\Psi_{p_1}\rangle|p_1\rangle$ is trapped in a harmonic potential by an electric field. If a measurement at $|p_2\rangle$ fails, the quantum

state collapsed to a maximally entangled state at $|p_1\rangle$.

-
- [1] R. Feynman, International Journal of Theoretical Physics **21**, 467 (1982).
- [2] A. K. Ekert, Phys. Rev. Lett. **67**, 661 (1991).
- [3] C. H. Bennett, G. Brassard, C. Crépeau, R. Jozsa, A. Peres, and W. K. Wootters, Phys. Rev. Lett. **70**, 1895 (1993).
- [4] C. H. Bennett and S. J. Wiesner, Phys. Rev. Lett. **69**, 2881 (1992).
- [5] D. P. DiVincenzo, Science **270**, 255 (1995).
- [6] R. Horodecki, P. Horodecki, M. Horodecki, and K. Horodecki, Rev. Mod. Phys. **81**, 865 (2009).
- [7] D. Collins, N. Gisin, and H. De Riedmatten, Journal of Modern Optics **52**, 735 (2005).
- [8] J. I. Cirac and P. Zoller, Nature **404**, 579 (2000).
- [9] C. H. W. Barnes, J. M. Shilton, and A. M. Robinson, Phys. Rev. B **62**, 8410 (2000).
- [10] E. Knill, R. Laflamme, and G. J. Milburn, Nature **409**, 46 (2001).
- [11] D. Loss and D. P. DiVincenzo, Phys. Rev. A **57**, 120 (1998).
- [12] M. A. Nielsen and I. L. Chuang, *Quantum Computation and Quantum Information* (Cambridge University Press, Cambridge, UK, 2000).
- [13] *IEEE International Conference on Computers, Systems and Signal Processing*, Vol. 175 (1984).
- [14] G. Brassard, N. Lütkenhaus, T. Mor, and B. C. Sanders, Phys. Rev. Lett. **85**, 1330 (2000).
- [15] P. Jouguet, S. Kunz-Jacques, A. Leverrier, P. Grangier, and E. Diamanti, Nature Photonics **7**, 378 (2013).
- [16] V. Vedral, *Introduction to Quantum Information Science* (Oxford University Press, Oxford, UK, 2006).
- [17] W. G. Unruh, Phys. Rev. A **51**, 992 (1995).
- [18] P. W. Shor, Phys. Rev. A **52**, R2493 (1995).
- [19] D. P. DiVincenzo and P. W. Shor, Phys. Rev. Lett. **77**, 3260 (1996).
- [20] D. G. Cory, M. D. Price, W. Maas, E. Knill, R. Laflamme, W. H. Zurek, T. F. Havel, and S. S. Somaroo, Phys. Rev. Lett. **81**, 2152 (1998).
- [21] D. P. DiVincenzo and P. W. Shor, Phys. Rev. Lett. **77**, 3260 (1996).
- [22] C. H. Bennett, D. P. DiVincenzo, J. A. Smolin, and W. K. Wootters, Phys. Rev. A **54**, 3824 (1996).
- [23] J.-W. Pan, C. Simon, C. Brukner, and A. Zeilinger, Nature **410**, 1067 (2001).
- [24] C. H. Bennett, G. Brassard, S. Popescu, B. Schumacher, J. A. Smolin, and W. K. Wootters, Phys. Rev. Lett. **76**, 722 (1996).
- [25] M. Murao, M. B. Plenio, S. Popescu, V. Vedral, and P. L. Knight, Phys. Rev. A **57**, R4075 (1998).
- [26] C. H. Bennett, H. J. Bernstein, S. Popescu, and B. Schumacher, Phys. Rev. A **53**, 2046 (1996).
- [27] P. G. Kwiat, S. Barraza-Lopez, A. Stefanov, and N. Gisin, Nature **409**, 1014 (2001).
- [28] See "Note added" in: C. H. Bennett, G. Brassard, and N. D. Mermin, Phys. Rev. Lett. **68**, 557 (1992).
- [29] U. Vazirani and T. Vidick, Phys. Rev. Lett. **113**, 140501 (2014).
- [30] *In Proceedings of the 39th Annual Symposium on Foundations of Computer Science, Palo Alto, 1998*, Vol. (IEEE, Washington, DC, 1998) (IEEE, 1998).
- [31] J. Barrett, L. Hardy, and A. Kent, Phys. Rev. Lett. **95**, 010503 (2005).
- [32] H.-K. Lo and N. Lütkenhaus, Physics in Canada **63** (2007).
- [33] S. D. Barrett and T. M. Stace, Phys. Rev. Lett. **105**, 200502 (2010).
- [34] R. Raussendorf and H. J. Briegel, Phys. Rev. Lett. **86**, 5188 (2001).
- [35] R. Raussendorf, D. E. Browne, and H. J. Briegel, Phys. Rev. A **68**, 022312 (2003).
- [36] O. Mandel, M. Greiner, A. Widera, T. Rom, T. W. Hansch, and I. Bloch, Nature **425**, 937 (2003).
- [37] M. Wallquist, K. Hammerer, P. Rabl, M. Lukin, and P. Zoller, Physica Scripta **2009**, 014001 (2009).
- [38] S. D. Barrett and P. Kok, Phys. Rev. A **71**, 060310 (2005).
- [39] P. van Loock, W. J. Munro, K. Nemoto, T. P. Spiller, T. D. Ladd, S. L. Braunstein, and G. J. Milburn, Phys. Rev. A **78**, 022303 (2008).
- [40] D. D. Awschalom, L. C. Bassett, A. S. Dzurak, E. L. Hu, and J. R. Petta, Science **339**, 1174 (2013), <http://www.sciencemag.org/content/339/6124/1174.full.pdf>.
- [41] S. E. Ahnert and M. C. Payne, Phys. Rev. A **71**, 012330 (2005).
- [42] E. T. Owen, M. C. Dean, and C. H. W. Barnes, Phys. Rev. A **85**, 022319 (2012).
- [43] E. T. Owen, M. C. Dean, and C. H. W. Barnes, Phys. Rev. A **89**, 032305 (2014).
- [44] R. Bowler, J. Gaebler, Y. Lin, T. R. Tan, D. Hanneke, J. D. Jost, J. P. Home, D. Leibfried, and D. J. Wineland, Phys. Rev. Lett. **109**, 080502 (2012).
- [45] G. Huber, T. Deuschle, W. Schnitzler, R. Reichle, K. Singer, and F. Schmidt-Kaler, New Journal of Physics **10**, 013004 (2008).
- [46] *On the Transport of Atomic Ions in Linear and Multidimensional Ion Trap Arrays*, Vol. 8 (2008).
- [47] J. H. Davies, I. A. Larkin, and E. V. Sukhorukov, Journal of Applied Physics **77** (1995).
- [48] W. M. Witzel, M. S. Carroll, A. Morello, L. Cywiński, and S. Das Sarma, Phys. Rev. Lett. **105**, 187602 (2010).
- [49] E. Abe, A. M. Tyryshkin, S. Tojo, J. J. L. Morton, W. M. Witzel, A. Fujimoto, J. W. Ager, E. E. Haller, J. Isoya, S. A. Lyon, M. L. W. Thewalt, and K. M. Itoh, Phys. Rev. B **82**, 121201 (2010).
- [50] M. Veldhorst, J. C. C. Hwang, C. H. Yang, A. W. Leenstra, B. de Ronde, J. P. Dehollain, J. T. Muhonen, F. E. Hudson, K. M. Itoh, A. Morello, and A. S. Dzurak, Nature Nanotechnology **9**, 981 (2014).
- [51] T. S. Santos, Phd thesis, MIT (2007).
- [52] M. Gimeno-Segovia, P. Shadbolt, D. E. Browne, and T. Rudolph, Phys. Rev. Lett. **115**, 020502 (2015).
- [53] D. E. Browne and T. Rudolph, Phys. Rev. Lett. **95**, 010501 (2005).
- [54] W. P. Grice, Phys. Rev. A **84**, 042331 (2011).
- [55] A. Goldberg, H. M. Schey, and J. L. Schwartz, American Journal of Physics **35**, 177 (1967).

- [56] J. J. V. Maestri, R. H. Landau, and M. J. Paez, American Journal of Physics **68**, 1113 (2000).
- [57] S. E. Kronin, *Computational Physics* (Benjamin Cummings, Reading, UK, 1986).
- [58] A. Askar and A. S. Cakmak, The Journal of Chemical Physics **68** (1978).